

# REPORT DOCUMENTATION PAGE

Form Approved OMB No. 0704-0188

Public reporting burden for this collection of information is estimated to average 1 hour per response, including the time for reviewing instructions, searching existing data sources, gathering and maintaining the data needed, and completing and reviewing the collection of information. Send comments regarding this burden estimate or any other aspect of this collection of information, including suggestions for reducing this burden to Washington Headquarters Services, Directorate for Information Operations and Reports, 1215 Jefferson Davis Highway, Suite 1204, Arlington, VA 22202-4302, and to the Office of Management and Budget, Paperwork Reduction Project (0704-0188), Washington, DC 20503.

1. AGENCY USE ONLY (Leave blank)		2. REPORT DATE 10 August 1999	3. REPORT TYPE AND DATES COVERED Final Report	
4. TITLE AND SUBTITLE Experimental Investigation of Supersonic Combustion of Liquid Hydrocarbon Fuel Using Barbotage in the Aeroramp Configuration at M=2.5			5. FUNDING NUMBERS F61775-98-WE118	
6. AUTHOR(S) Dr. Vladimir Sabelnikov				
7. PERFORMING ORGANIZATION NAME(S) AND ADDRESS(ES) TsAGI Zhukovsky St Moscow 140160 Russia			8. PERFORMING ORGANIZATION REPORT NUMBER N/A	
9. SPONSORING/MONITORING AGENCY NAME(S) AND ADDRESS(ES) EOARD PSC 802 BOX 14 FPO 09499-0200			10. SPONSORING/MONITORING AGENCY REPORT NUMBER SPC 98-4078	
11. SUPPLEMENTARY NOTES				
12a. DISTRIBUTION/AVAILABILITY STATEMENT Approved for public release; distribution is unlimited.			12b. DISTRIBUTION CODE A	
13. ABSTRACT (Maximum 200 words)  This report results from a contract tasking TsAGI as follows: The contractor will investigate combustion of kerosene using barbotage by hydrogen and air in the aeroramp configuration at M=2.5 as described in his proposal dated 1 Jun 98.				
19991005 112				
14. SUBJECT TERMS EOARD, Combustion, Supersonic Injection			15. NUMBER OF PAGES 35	
			16. PRICE CODE N/A	
17. SECURITY CLASSIFICATION OF REPORT UNCLASSIFIED	18. SECURITY CLASSIFICATION OF THIS PAGE UNCLASSIFIED	19. SECURITY CLASSIFICATION OF ABSTRACT UNCLASSIFIED	20. LIMITATION OF ABSTRACT UL	

NSN 7540-01-280-5500

Standard Form 298 (Rev. 2-89)  
Prescribed by ANSI Std. Z39-18  
298-102

**DTIC QUALITY INSPECTED 4**

Central Aerohydrodynamic Institute  
TsAGI  
Zhukovsky, Moscow region, Russia

" 10 " August 1999

Final report

**Experimental Investigation of Supersonic Combustion of  
Liquid Hydrocarbon Fuel Using Barbotage in the Aeroramp  
Configuration at  $M=2.5$**

Contract F61775-98-WE118,

SPC 98-4078, Air Force Office of Scientific Research (AFOSR), USA

**Principal Investigator**



**Vladimir Sabel'nikov**

**Authors**

Voloschenko O., senior research engineer

Ivanov V., Ph. Doctor

Korontsvit Yu., Ph. Doctor

Nikolaev A., research engineer

Sabel'nikov V., professor

Zosimov S., research engineer

AQFOO-01-2486

## Contents

	Page
Abstract	3
1. Introduction	4
2. Experimental facility	6
3. Supersonic combustor	7
4. Injectors	8
5. Test methodology and instrumentation	9
6. Test results	10
7. Conclusions	14
References	15
Table	16
Figure captures	18

## **Abstract**

Results of investigations of combustion of liquid hydrocarbon fuel jets aerated by hydrogen or air in a supersonic flow in the two-dimensional diverging-area supersonic combustor are presented. Direct-connect combustor tests were conducted at the combustor entrance Mach number  $M=2.5$  and total temperature in the range of  $T=1660-1798K$ . The liquid hydrocarbon fuel supply into the combustor was executed through the aeroramp configuration (four tests) and tube-micropylons with circular nozzles (three tests; baseline results) installed at the angle of 45 degrees with respect to the mainstream air flow direction.

## 1.Introduction

The first stage of the investigation of the supersonic mixing and combustion enhancement technique which was supported by NAVY USA, Office of Naval Research contract No. N00014-96-1-0869, was carried out in cooperation with Dr. Klaus Schadow and with Dr. Gabriel D. Roy, as the technical monitor. The objective of that investigation was to study potential possibilities of supersonic mixing and combustion enhancement using liquid hydrocarbon fuel aerated by gas (hydrogen or air) injected through noncircular nozzles. The fuel was injected through elliptical and circular (baseline configuration) nozzles from injectors of two geometries: tube-micropylons and fin-pylons. The following results were obtained [1]:

- elliptical nozzles provided greater mixing and combustion efficiencies in comparison with round nozzles for the cases when the liquid hydrocarbon fuel aerated by gas was injected from the tube-micropylons at the angle of 45 degrees relative to the mainstream air flow direction;
- injection from the tube-micropylons at the angle of 45 degrees relative to the mainstream air flow direction provided greater mixing and combustion efficiencies in comparison with the co-flow injection from the fin-pylons;
- test results obtained for the fin-pylons with the co-flow injection of the liquid hydrocarbon fuel aerated by gas did not show noticeable difference in mixing and combustion efficiencies for round and elliptical nozzles;
- aeration of the liquid hydrocarbon fuel by gas considerably intensified supersonic mixing and combustion in the scramjet combustor.

Obtained results as a whole showed the good prospect of using effervescent liquid hydrocarbon fuel sprays in order to intensify supersonic mixing and combustion in the scramjet combustor.

In the course of discussions concerning the results of the first stage of the

investigation Dr. Lee Bain and Dr. Thomas Jackson (AFRL/PRSS) suggested to continue the investigations in this direction. Dr. Thomas Jackson suggested in the future tests to use "gas wedges" (aeroramp configuration), formed by injection of the liquid hydrocarbon fuel, barbotaged by gas.

The idea of aeroramp as a way of the fuel supply was proposed in [2,3]. The paper [3] presents the results of investigations of fuel jets injection with different impulses from walls through variable area orifices. The specific combination of jets intensity and orifices areas permits to obtain a flow field close in structure to the field of supersonic flow around a solid wedge and to reach the increase of jets penetration. Further evolution of the idea of using gas jets for intensification of mixing consists in choosing the way of "gas wedges" formation, e.g., using different directions of injection of jets placed locally (the aeroramp configuration). Herewith, similarity of the flowfield around the solid wedge (the NASA ramp) with the characteristic disposition of shock waves and vortical separation zones is achieved in the external supersonic flow.

The aim of the present second stage of the work (which is done in the frame of the contract F61775-98-WE118 with AFOSR, USA) is to study the supersonic mixing and combustion enhancement in the scramjet combustor using the liquid hydrocarbon fuel jets aerated by hydrogen or air in the aeroramp configuration (Dr. Thomas Jackson suggestion).

This second stage with the aeroramp was carried out at TsAGI test facility T-131B using the direct-connect tests. The intermediate results of the work were presented in the first and second interim reports [5,6].

The final report summarizes the description of the test facility (paragraph 2), supersonic combustor model (paragraph 3), injectors (paragraph 4), tests methodology and instrumentation (paragraph 5), results of tests, their analysis and discussions (paragraph 6). Conclusions are given in paragraph 7.

## 2. Experimental facility

The experimental investigation of combustion of liquid hydrocarbon fuel jets aerated by gas (air or hydrogen) was performed in the direct-connect facility of TsAGI T-131B. Kerosene-air vitiated heater with oxygen replenishment was used to provide the high enthalpy flow with the desired values of the stagnation pressure  $P_t$  and the stagnation temperature  $T_t$  and the mass fraction of free oxygen  $Y_{O_2}$  (23%).

The kerosene combustion efficiency in the heater was close to 1. The estimates based on the results of numerical calculations show that the combustion products from the heater at  $T_t \leq 2000$  K practically consist of  $CO_2$ ,  $H_2O$ ,  $N_2$ ,  $O_2$ , i.e. there is no dissociation. A summary of the total flow parameters and other parameters characterizing the facility and combustor operation regimes are given in Table No.1.

Figure 1 shows the scheme of the facility and supersonic combustor. Kerosene was supplied into the heater through a two-dimensional fuel manifold equipped with rotary-type injectors (discharge nozzles) for spraying the liquid fuel.

The oxygen and air were supplied into the heater through the Venturi-type nozzles with the nozzle throat diameters of 7.5 and 14.4 mm, respectively. The choice of such sizes of the Venturi-type nozzles is specified by providing the oxygen mass fraction of 23% in the heater at the gas stagnation temperature  $T_t=1700$  K.

To generate a supersonic flow at the combustor entry, a two-dimensional Mach 2.5 nozzle was used. The throat dimensions of the nozzle are  $10.6 \times 100$  mm<sup>2</sup> and the exit section dimensions are  $30 \times 100$  mm<sup>2</sup>. The nozzle was designed by the method of characteristics for the Mach number  $M = 2.5$ , the ratio of specific heats used for calculations was taken equal 1.33. The constructions of the heater and nozzle are cooled by water.

## 3. Supersonic combustor

The schematic view of the combustor is shown in Fig.2. The combustor duct

consisted of 4 sections (6 segments) bolted together:

- the first was 150 mm long with the constant area section of  $30 \times 100 \text{ mm}^2$  (one segment);
- the second was 150 mm long with the divergence angle of 3.0 degree along the upper wall, exit cross-area section is  $37.8 \times 100 \text{ mm}^2$  (one segment);
- the third was 300 mm long with the divergence angle of 2.3 degree along the upper wall, exit cross-area section is  $49.9 \times 100 \text{ mm}^2$  (one segment);
- the fourth was 450 mm long with the constant cross-area section of  $49.9 \times 100 \text{ mm}^2$  (3 segments, each of them 150 mm long).

The total length of the combustor was 1050 mm, the area-expansion ratio of the combustor was 1.67. The combustor is smoothly attached to the nozzle, since the cross-area section of the combustor duct entry coincides with the rectangular exit nozzle section with dimensions of  $30 \times 100 \text{ mm}^2$ . The combustor cross-section (beginning from the distance 50 mm from the entrance section) has round corners, the radius of rounding is 5 mm. The combustor walls were uncooled, they are made of heat-resistant steel, the wall thickness is 8 mm. The combustion times during test runs did not exceed 6 seconds to avoid excessive wall temperatures.

The upper and lower walls of the combustor are drained by the holes (46 locations) for measuring the static pressure on the wall along the combustor with a spacing of 30–50 mm.

At the lower wall there are also holes along the combustor duct for installation of heat flux sensors.

An exhaust diffuser (into which the vertical 5-point pitot pressure rake cooled by water was installed) can be attached to the last segment of the combustor. The last segment of the combustor is equipped with a manifold (collector) for a normal injection of air jets into the combustor duct that allows us to perform the combustor flow throttling that is necessary for establishing conditions for the fuel ignition and combustor start.

The front combustor segment has a hatch on the upper wall, dimensions of which are  $80 \times 90 \text{ mm}^2$ . Different types of injectors for fuel supply can be installed at the hatch cover.

#### 4. Injectors

Two kinds of injectors for supplying the liquid hydrocarbon fuel jets aerated by gas were investigated:

- aeroramp-type injectors;
- tube-injectors with circular holes-nozzles of the diameter  $d=1.2 \text{ mm}$ .

Two aeroramp-injectors were installed at the upper combustor wall at the distance of 95 mm from the combustor entrance and 25 mm from the side walls. The installation scheme of the aeroramp at the cover and location of each of 9 holes-injectors of the diameter  $d=0.6 \text{ mm}$  are presented in Fig.3. The relative disposition of the holes in the group, as well as three-dimensional orientation of their axes relative to the operating surface of the insert mounted flush with the plane of the cover define the direction of propagation (injection) of aerated jets in accord with the proposed scheme of the gas wedge forming.

Four tube-injectors were installed at the upper combustor wall at the distance of 95 mm from the combustor entrance with the spacing of 24 mm between them and the last left and right ones were located at the distance of 14 mm from the side walls. The installation scheme of the tube-injectors at the cover is presented in Fig.4.

The liquid hydrocarbon fuel jets were aerated by air or hydrogen, the mass fraction of gas used for aeration was  $\leq 0.1$  for air and  $\leq 0.025$  for hydrogen.

#### 5. Tests methodology and instrumentation

Test runs were performed in the following sequence:

- cold air supply through injectors (for protection aims) is switched on;

- the data acquisition system is switched on;
- the air-heater is switched on and the required conditions with respect to the stagnation pressure  $P_t$  and temperature  $T_t$  are attained;
- the fuel supply into the combustor is switched on to reach the desired regime (the cold air supply through injectors is switched off during the fuel supply and again is switched on after the fuel supply stoppage);
- the kerosene-air mixture is ignited using an air jet pulse (0.5-1 s) through a flush wall injector located at the end combustor segment (pulsed combustor throttling);
- after ignition and reaching the steady combustion process the fuel supply is continued during 5-6 s, minimum fuel equivalence ratios ER at which the extinction of the flame take place (i.e. fuel lean blow out limit) were determined by continuous decreasing of the kerosene mass rate.

During tests the following parameters were measured:

- longitudinal distributions of static pressures along the walls of the combustor;
- heat fluxes to the walls along the duct length;
- total pressure at the exit section;
- pressure in the fuel manifold and mass rate of fuel;
- pressure and temperature of oxygen before the Venturi tube;
- pressure and temperature of air before the Venturi tube;
- pressure and mass rate of kerosene before the fuel collector of the air-heater;
- pressure in the air-heater.

The scheme of measurements for the combustor model and the test facility, as well as the ranges, measuring devices are given in Fig.5.

Visualization of the flow pattern and fuel mixture sprays in the supersonic flow at the combustor exit included two video-systems: schlieren system in the horizontal plane and the colour video-system in vertical plane.

## 6. Test results

Seven test runs were performed (see Table No.1). Test runs No.1-No.4 were conducted with aeroramp-type injectors and test runs No.5-No.7 with tube-micropylons (the basic configuration). In tests No.1, No.4, No.5 and No.7 the jets of the liquid hydrocarbon fuel were aerated by air, and in tests No.2, No.3, and No.6 jets of the fuel were aerated by hydrogen. In the test run No.3 the vertical total pressure rake was installed at a distance of 900 mm from the combustor entrance.

In test runs No.4 and No.7 visualization of the liquid hydrocarbon fuel jets aerated by air and injected through the aeroramp-injector and tube-injector was performed without combustion. The injectors were installed at the combustor exit at the distance of 900 mm from the combustor entrance, ensuring the possibility to perform the visualization in the free flow.

Figs.6 and 7 show the axial normalized pressure (the ratio of the static pressure to the heater pressure) distributions on the combustor walls for the aeroramp-injectors, in the test run No.1 (fuel aerated by air) and in the test run No.2 (fuel sprays aerated by hydrogen).

Figs.8 and 9 show the normalized static pressure distributions along the combustor walls for the test run No.5 (aeration of fuel jets by air) and in the test run No.6 (aeration of fuel jets by hydrogen) for tube-injectors.

The heat flux distributions measured along the lower wall of the combustor in the experiments with the aeroramp- and tube-injectors are presented in Figs.10,11.

It is seen from Figs.6-9 that for no fuel supply into the combustor (i.e. for fuel equivalence ratio  $ER=0$ ) the supersonic flow is observed along the entire length of the combustor duct. In the rear part of the combustor, due to the flow overexpansion, flow separation took place.

In the tests with fuel injection and combustion the pressure starts to increase some

distance downstream of the fuel injectors, demonstrating the induction delay.

For aeroramp-injectors, as is seen from the wall pressure distributions along the combustor, the combustion intensity practically did not depend on the type of the gas used for aeration (see the test run 1,  $ER=0.65$  - aeration by air, Fig.6 and the test run 2,  $ER=0.66$  - aeration by hydrogen, Fig.7).

The aeroramp configuration provides smaller combustion efficiency as compared with the tube-injectors. For example, for practically the same values of  $ER$  the maximum level of the normalized static pressure for the aeroramp-injectors exceeds the one for the tube injectors:  $(P/P_t)_{max}=0.165$  at  $ER=0.66$  (Fig.6) and for the tube-injectors  $(P/P_t)_{max}=0.2$  at  $ER=0.65$  (Fig.8).

From the heat flux distributions to the walls of the divergent part of the combustor (presented in Figs.10 and 11) it is seen that the heat flux magnitudes for aeroramp configuration are considerably lower than for the tube-injectors:  $q_w=1.3 \times 10^6$  and  $q_w=1.7 \times 10^6$  W/m<sup>2</sup> for aeroramps and tubes, respectively, at  $ER \approx 0.65$ . The lower magnitudes of heat fluxes can be explained by decreasing the mixing and combustion intensities for the aeroramp-injectors in comparison with the tube injectors.

The total pressure measurements at the distance of 900 mm from the entrance, presented in Fig.12 (which were carried out by means of the rake) show that the large asymmetry of the flow took place due to combustion located mainly in the vicinity of the upper wall of the combustor for the aeroramp configuration.

The flow patterns with the liquid hydrocarbon fuel jets aerated by gas (Figs.13 and 14) show that the aeroramp configuration results in the penetration of the fuel in the transverse direction around of 10 mm height relative to injector wall. The flow patterns around the aeroramp-injector are similar to the wedge injectors investigated in [7].

The tube-injectors result in the quasi-uniform vertical distribution in the layer of 30 mm height, relative to injector wall.

Aeroramp-injectors provide a larger domain of stable combustion in comparison with the tube-injectors. The lean blowouts were sudden ones for both kinds of injectors, but stable combustion took place up to  $ER=0.32$  for aeroramp-injectors and up to  $ER=0.4$  for tube-injectors (Figs.6-9). The sudden lean blowout is illustrated in Fig. 15, where two successive flow patterns at decreasing the mass fuel rate are presented. The time interval between them was  $1/25$  s. For  $ER=0.32$  combustion took place, for  $ER=0.31$  blowout occurred. It has to be noted that the pressure distributions in the rear part of the combustor (presented in Figs.6 -9) for the blowout cases for the aeroramp-injectors at  $ER=0.31$  and tube-injectors at  $ER=0.39$  cannot be considered as the true ones because of the measurement system lag.

The estimation of the efficiency of the combustion and mixing of the liquid hydrocarbon fuel jets aerated by gas was carried according to the increment of the axial component of the integrated inner pressure force and the combustion efficiency (see details in [1,7]). The increment of the axial component of the integrated inner pressure force was determined from the measured (with and without combustion) static pressure distributions using the following relationship:

$$\Delta F = w \int (P_{comb} - P_{nocomb}) \sin \theta dx, \quad (1)$$

where  $\theta$  is the local wall angle with respect to the flow direction,  $x$  is the axial coordinate,  $w$  is the duct width. The figure 16 presents the normalized increments of the axial component of the integrated inner pressure force (with respect to the input flow impulse) induced by the combustion (for the aeroramp- and tube-injectors),  $\Delta \bar{F} = \Delta F / I_1$ , where  $I_1 = (P + \rho V^2) h w$  the total gasdynamic impulse at the combustor entrance. From Fig.16 it is seen that the  $\Delta \bar{F}$  increases with the growth of the ER and for the tube injectors it is considerably higher than for the aeroramp-injectors, the influence of the kind of gas used for aeration is insignificant.

The combustion efficiency was calculated by using a one-dimensional methodology [8] based on the solution of the equations of energy, mass and momentum

conservation at the known experimental values of the pressure distribution along the combustor walls (pressure was assumed to be constant across the duct section). The calculated combustion efficiency and mass-averaged flow parameters Mach number  $M$  and total pressure losses  $\sigma$  for the section at the distance of 900 mm from the combustor entrance are given in Table 2. The combustion efficiency was within 0.7-1.0 for the aeroramp-injectors at  $ER=0.32-0.79$  and 0.9-1.0 for the tube-injectors at  $ER=0.4-0.66$ .

## 7. Conclusions

The experimental study of the combustion of the liquid hydrocarbon fuel jets aerated by hydrogen or air were performed in the two-dimensional diverging-area supersonic combustor with the use of two types of injectors: the aeroramps and tubes. The experiments were performed at the following flow parameters at the combustor inlet: Mach number  $M=2.5$ , the stagnation temperature  $T_t=1660-1798$  K, stagnation pressure  $P_t=1.73-1.78$  MPa, the mass fraction of free oxygen  $Y_{O_2} = 0.22-0.24$ .

The following results were obtained:

1. Aeroramp-injector forms the flow pattern similar to a one around the wedge injector.
2. The fuel supply through the aeroramp-injectors results in a quite large nonuniformities in vertical fuel distribution in the combustor duct with the maximum fuel concentration in the proximity of the wall at which aeroramps were installed.
3. The aeroramp-injectors result in less intense combustion process in comparison with the tube-injectors.
4. The aeroramp-injectors provide a larger domain of the stable combustion in comparison with the tube-injectors.
5. Type of gas (air or hydrogen) used for aeration of the liquid hydrocarbon fuel jets has a minor influence on the intensity of the mixing and combustion in the supersonic combustor.

## References

1. V.A.Sabel'nikov et al. Investigation of supersonic combustion enhancement using barbotage and injectors with noncircular nozzles. AIAA Paper 98-1516, p.10, 1998.
2. R.E.Breidenthal. Exponential pulse method and apparatus. 1986, US Patent applications 06/912, 795.
3. P.Clement, C.Rodriguez. Shock wave structure and penetration height in transverse jets. AIAA Paper 89-0841, 1989.
4. V.N. Avrashkov, S.I. Baranovsky, D.M. Davidenko. Penetration height of a liquid jet saturated by gas bubbles. Izvestiya VUZov, Aviatsionnaya tekhnika, 1990, No.4, pp. 96-98.
5. V.A.Sabel'nikov et al. Experimental Investigation of Supersonic Combustion of Liquid Hydrocarbon Fuel Using Barbotage in the Aeroramp Configuration at  $M=2.5$ . 1st quarterly report on Contract F61775-98-WE118, SPC 98-4078, Air Force Office of Scientific Research (AFOSR), USA, 1998.
6. V.A.Sabel'nikov et al. Experimental Investigation of Supersonic Combustion of Liquid Hydrocarbon Fuel Using Barbotage in the Aeroramp Configuration at  $M=2.5$ . 2nd quarterly report on Contract F61775-98-WE118, SPC 98-4078, Air Force Office of Scientific Research (AFOSR), USA, 1999.
7. Scott D. Stouffer, Uri Vandsburger, G.Burton Northam. Comparison of Wall Mixing Concepts for Scramjet Combustors, AIAA Paper 94-0587, p.12, 1994.
8. V.A.Sabel'nikov et al. Investigation of Supersonic Combustion Enhancement Using Barbotage and Injectors with Noncircular Nozzles. Final report on Contract NAVY USA ONR 000014-96-1-0869, 1997.

Table No1. Test conditions

Run number	Aeration gas	$P_t$ , MPa	$T_T$ , k	$Y_{O_2}$	ER
<b>Injectors-aeroramp</b>					
1	air	1.75	1684	0.238	0
-"-	-"-	1.74	1660	0.226	0.79
-"-	-"-	1.72	1700	0.239	0.47
-"-	-"-	1.73	1678	0.244	0.35
-"-	-"-	1.74	1700	0.242	0.33
2	hydrogen	1.71	1717	0.227	0
-"-	-"-	1.73	1731	0.229	0.67
-"-	-"-	1.73	1711	0.241	0.32
3*	hydrogen	1.78	1752	0.236	0
-"-	-"-	1.78	1798	0.237	0.62
4**	air	2.52	1435	0.122	0.42
<b>Tube-injectors</b>					
5	hydrogen	1.73	1692	0.243	0
-"-	-"-	1.73	1680	0.220	0.60
-"-	-"-	1.73	1691	0.242	0.39
6	hydrogen	1.73	1700	0.240	0
-"-	-"-	1.73	1738	0.241	0.41
7**	air	2.52	1438	0.124	0.65-0.7

\* - run with rake at X=900 mm section from combustion entrance

\*\* - run with visualization of jets

 $Y_{O_2}$  - oxygen mass fraction in heater gas

ER - equivalence ratio

 $P_{mix}$  - pressure of injection $Y_{bar}$  - barbotage mass fraction (C

Table No2. Flow parameters at the distance  $x=900$  mm from the combustor entrance

Run number	Injectors	Aeration gas	ER	$\eta$ (combustion efficiency)	M
1	aeroramp	air	0.79	0.8	1.0
"-	"-	"-	0.65	0.69	1.0
"-	"-	"-	0.33	0.89	1.0
2	"-	hydrogen	0.66	0.69	1.0
"-	"-	"-	0.32	0.95	1.0
3	"-	"-	0.62	0.72	1.0
5	tubes	air	0.66	0.92	1.0
"-	"-	"-	0.4	0.99	1.0
6	"-	hydrogen	0.41	1.0	1.0

## Figure captures

Fig.1 Scheme of the test facility.

Fig.2 Schematic view of the model combustor.

Fig.3 Installation scheme of the aeroramps at the cover.

Fig.4 Installation scheme of the tube pylons at the cover.

Fig.5 Scheme of measurements for the combustor and test bed.

Fig.6 Wall pressure distributions along the combustor for aeroramps; aeration by air.

Fig.7 Wall pressure distributions along the combustor for aeroramps; aeration by hydrogen.

Fig.8 Wall pressure distributions along the combustor for tube pylons; aeration by air.

Fig.9 Wall pressure distributions along the combustor for tube pylons; aeration by hydrogen.

Fig.10 Heat flux distribution along the bottom combustor wall for the test run 11 (fig.6).

Fig.11 Heat flux distribution along the bottom combustor wall for the test run 15 (fig.8).

Fig.12 The total pressure profile at the combustor exit section; aeroramps, aeration by hydrogen.

Fig.13 Flow pattern of fuel jets aerated by air in supersonic flow, injection through aeroramps ( $G_{\text{fuel}} \sim 20\text{g/s}$ ,  $M=2.5$ ,  $T_t=1435\text{K}$ ,  $P=0.1\text{ Mpa}$ ).

Fig.14 Flow pattern of fuel jets aerated by air in supersonic flow, injection through tube pylons ( $G_{\text{fuel}} \sim 18\text{g/s}$ ,  $M=2.5$ ,  $T_t=1438\text{K}$ ,  $P=0.1\text{ Mpa}$ ).

Fig.15 Video-recording of the flow pattern at the combustor exit for modes of burning and blowout.

Fig.16 Comparison of normalized combustion induced pressure-area

integrals for aeroramps and tube-micropylons.



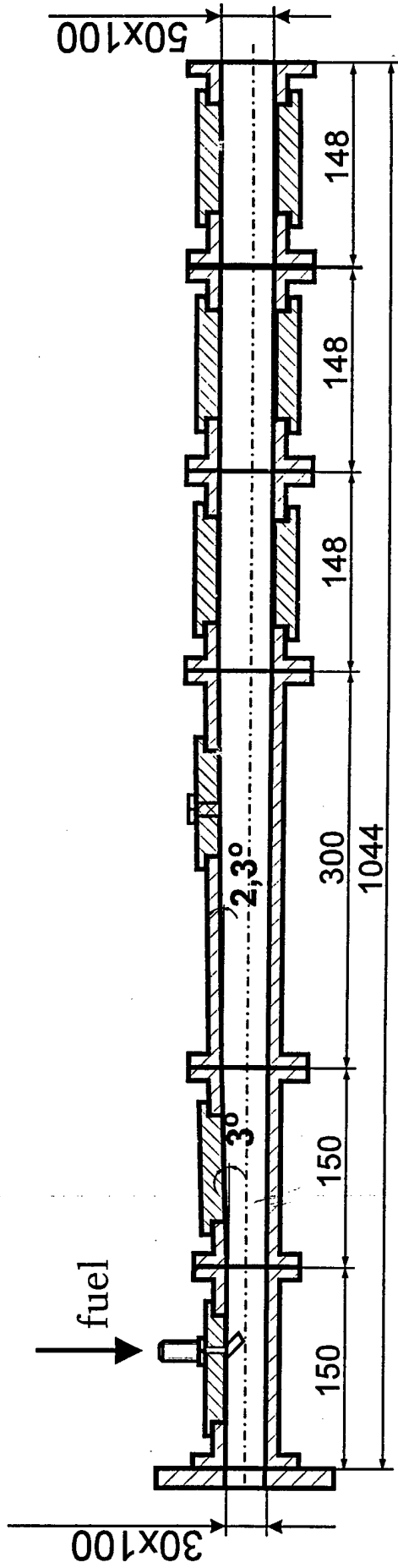
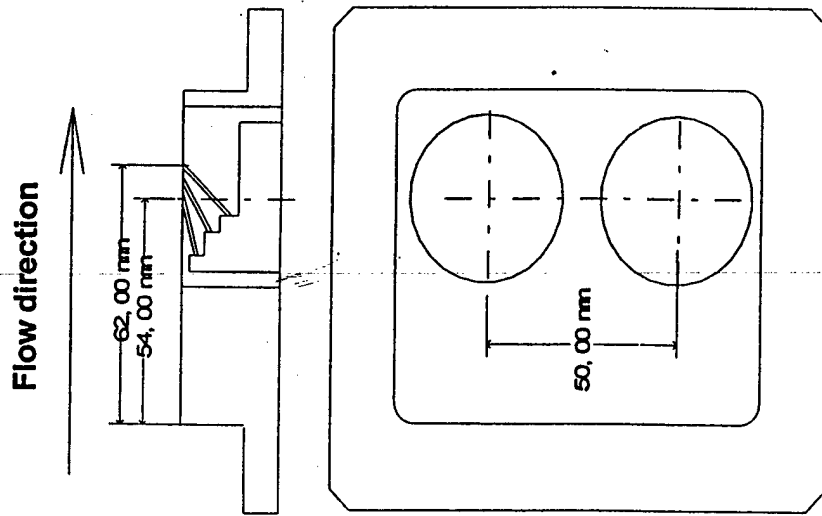


Fig. 2



Hole No.	Diameter, mm	Inclination, degree	Yaw, degree
1.	0.57	15	0
2.	0.57	15	0
3.	0.57	15	0
4.	0.57	30	-15
5.	0.57	30	0
6.	0.57	30	+15
7.	0.57	45	-30
8.	0.57	45	0
9.	0.57	45	+30

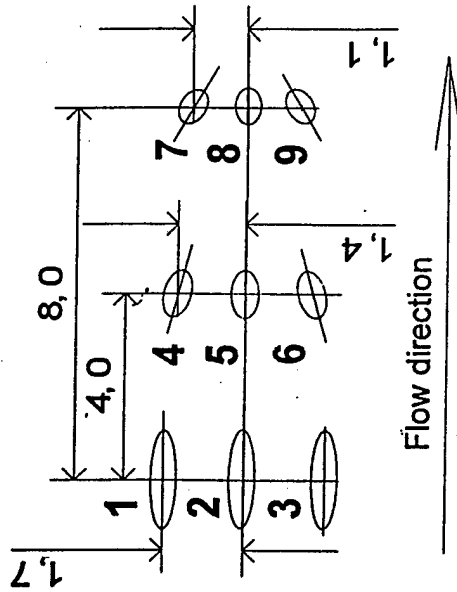


Fig.3

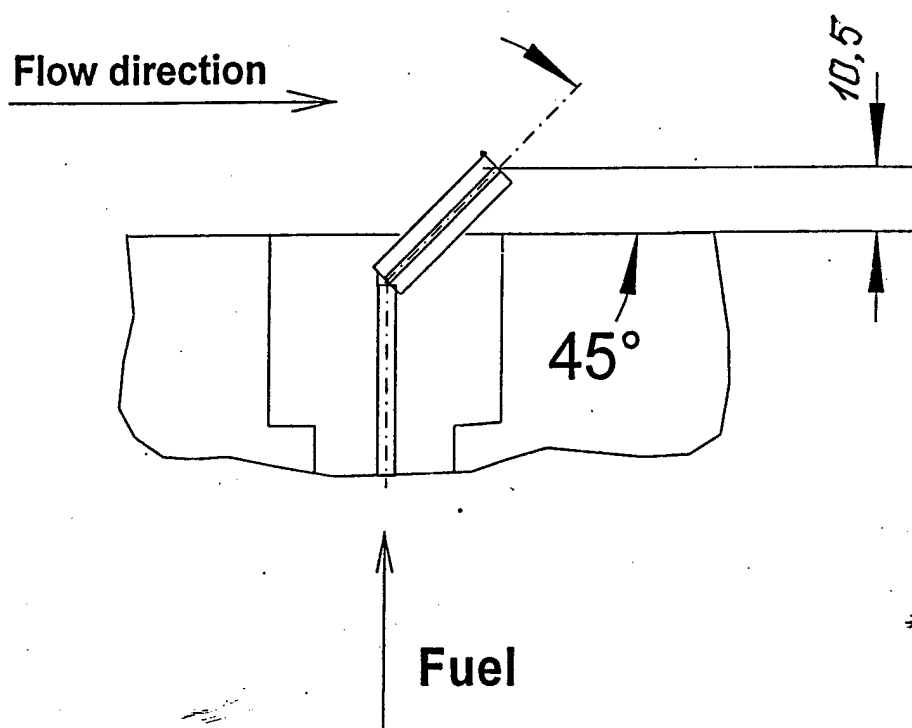
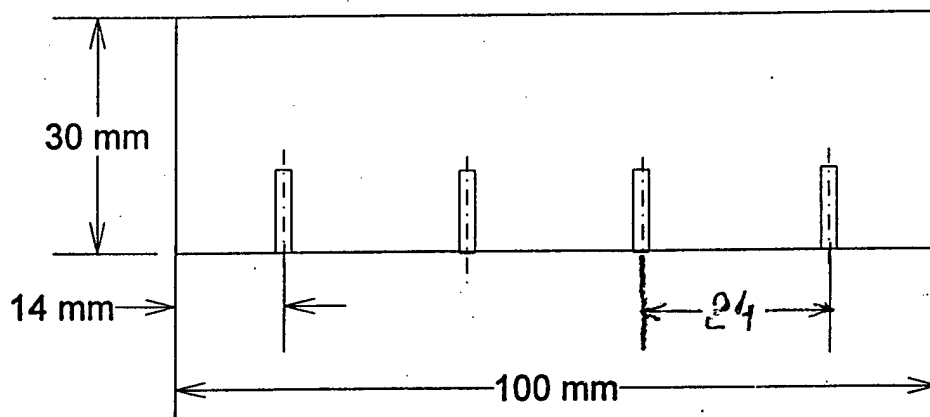
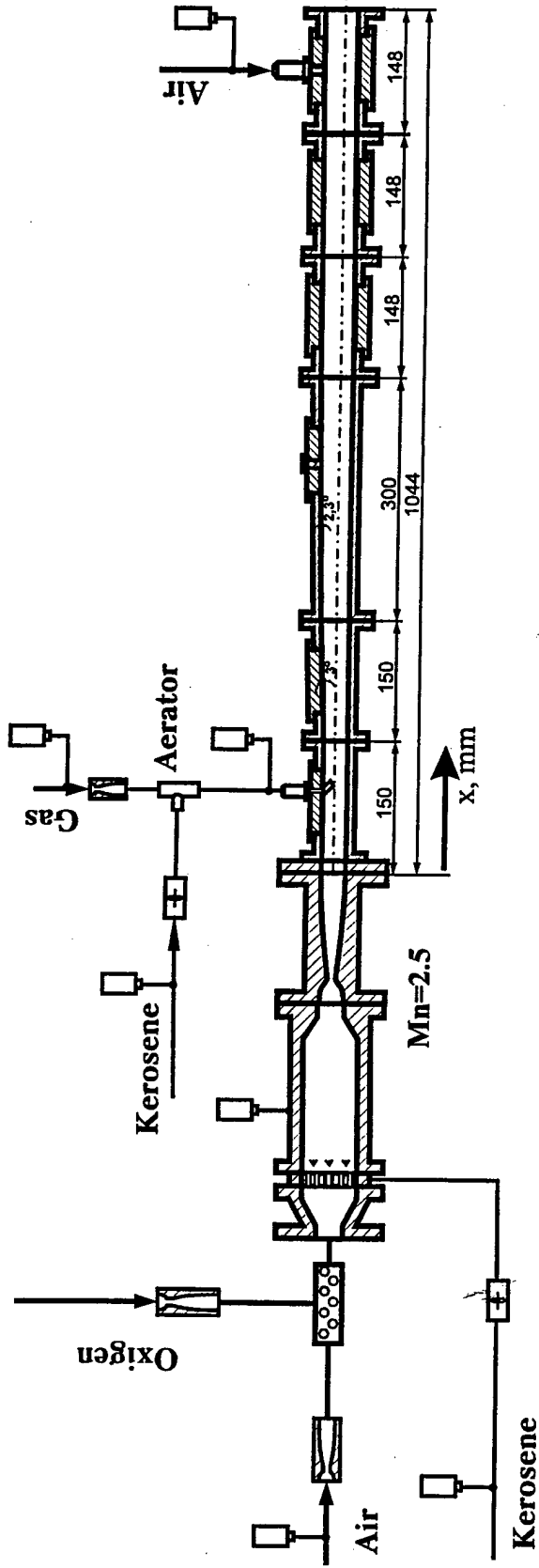


Fig. 4



### heat flux sensors

Number of measurement point	1	2	3	4
distance from the nozzle exit, mm	75	260	420	570
	bottom wall			

### pressure sensors

Number of measurement point	1	2	3	4	5	6	7	8	9	10	11	12	13	14	15	16	17	18	19	20	21	22	23	24	25	26
distance from the nozzle exit, mm	30	60	90	120	180	210	240	270	330	360	390	420	450	480	510	540	570	644	674	704	792	822	852	946	996	1039
	bottom wall																									

Number of measurement point	27	28	29	30	31	32	33	34	35	36	37	38	39	40	41	42	43	44	45	46	
distance from the nozzle exit, mm	37	55	55	60	65	70	80	95	180	210	240	330	360	390	420	570	792	822	852	894	
	upper wall																				

Fig. 5.

Test No1. aeroramps, aeration by air

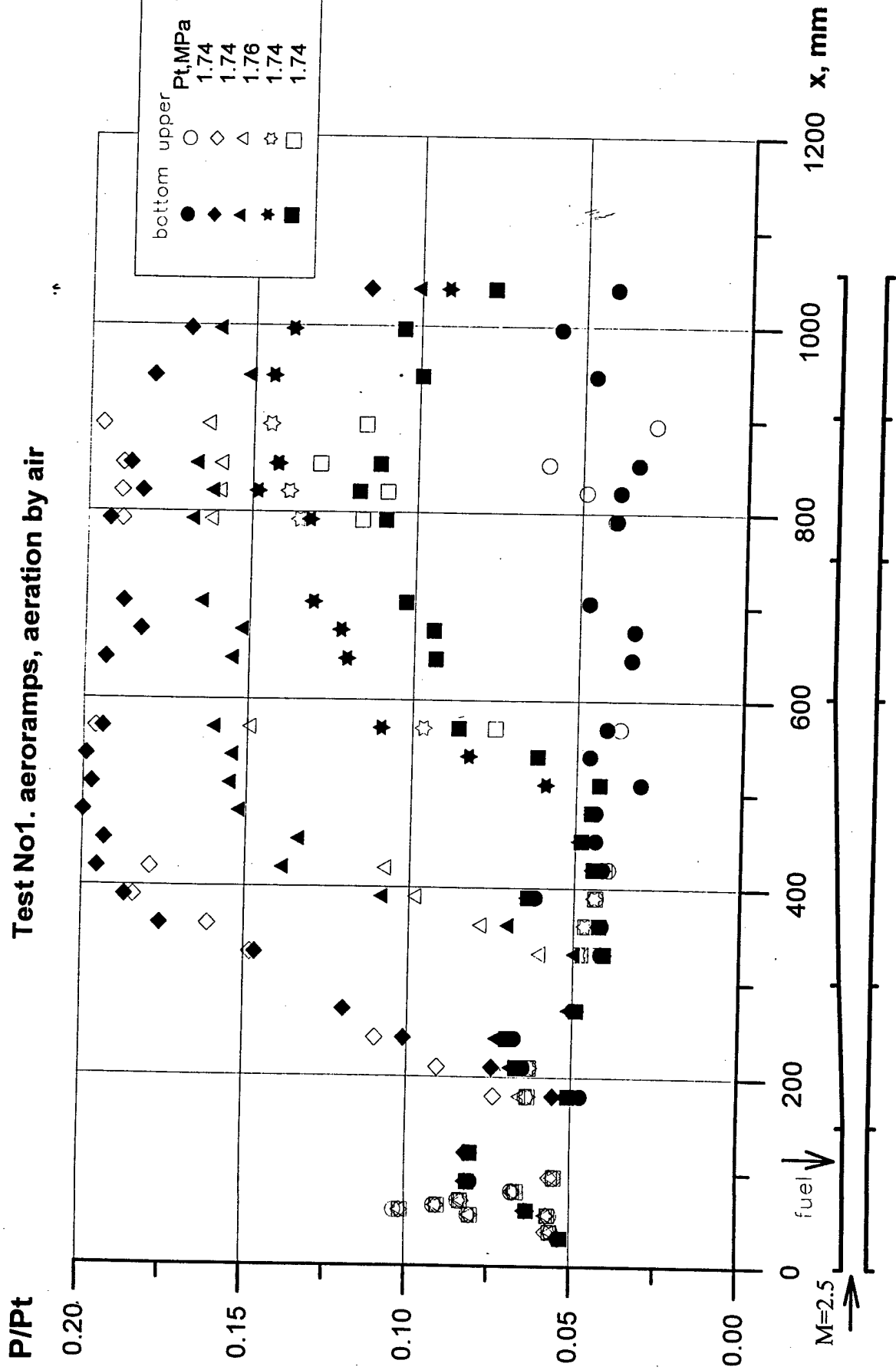


Fig. 6.

Test No2. aeroramps, aeration by hydrogen

P/Pt

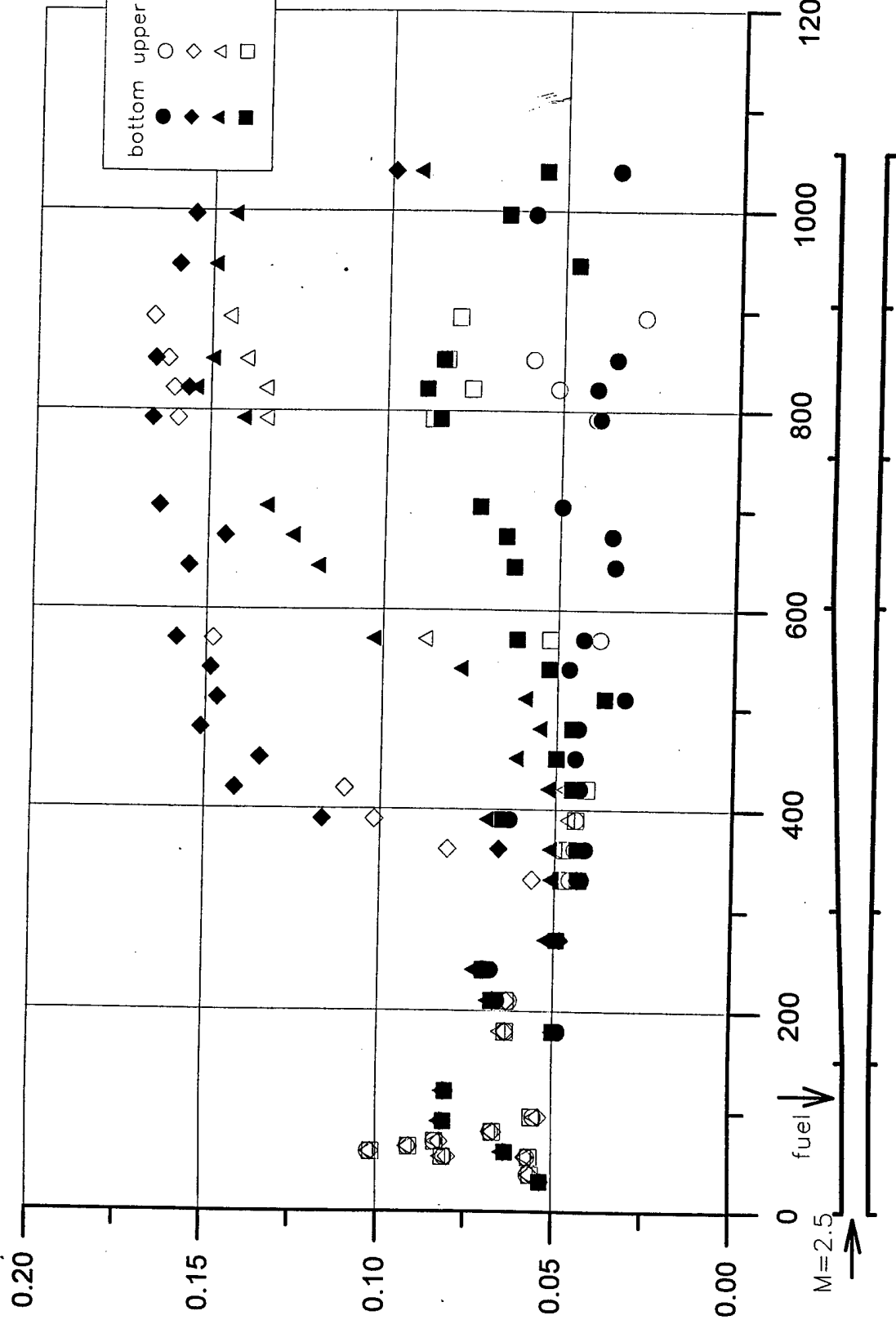


Fig. 7.

Test No5. tube injectors, aeration by air

P/Pt

0.20

0.15

0.10

0.05

0.00

M=2.5  
fuel ↓

200

400

600

800

1000

1200

x, mm

bottom		upper	
●	○	○	○
◆	◇	◇	◇
▲	△	△	△
■	□	□	□

Pt,MPa	Tt,K	ER
1.73	1692	0
1.73	1680	0.66
1.73	1691	0.40
1.73	1690	0.39

Fig. 8.

Test No6. tube injectors, aeration by hydrogen

P/Pt

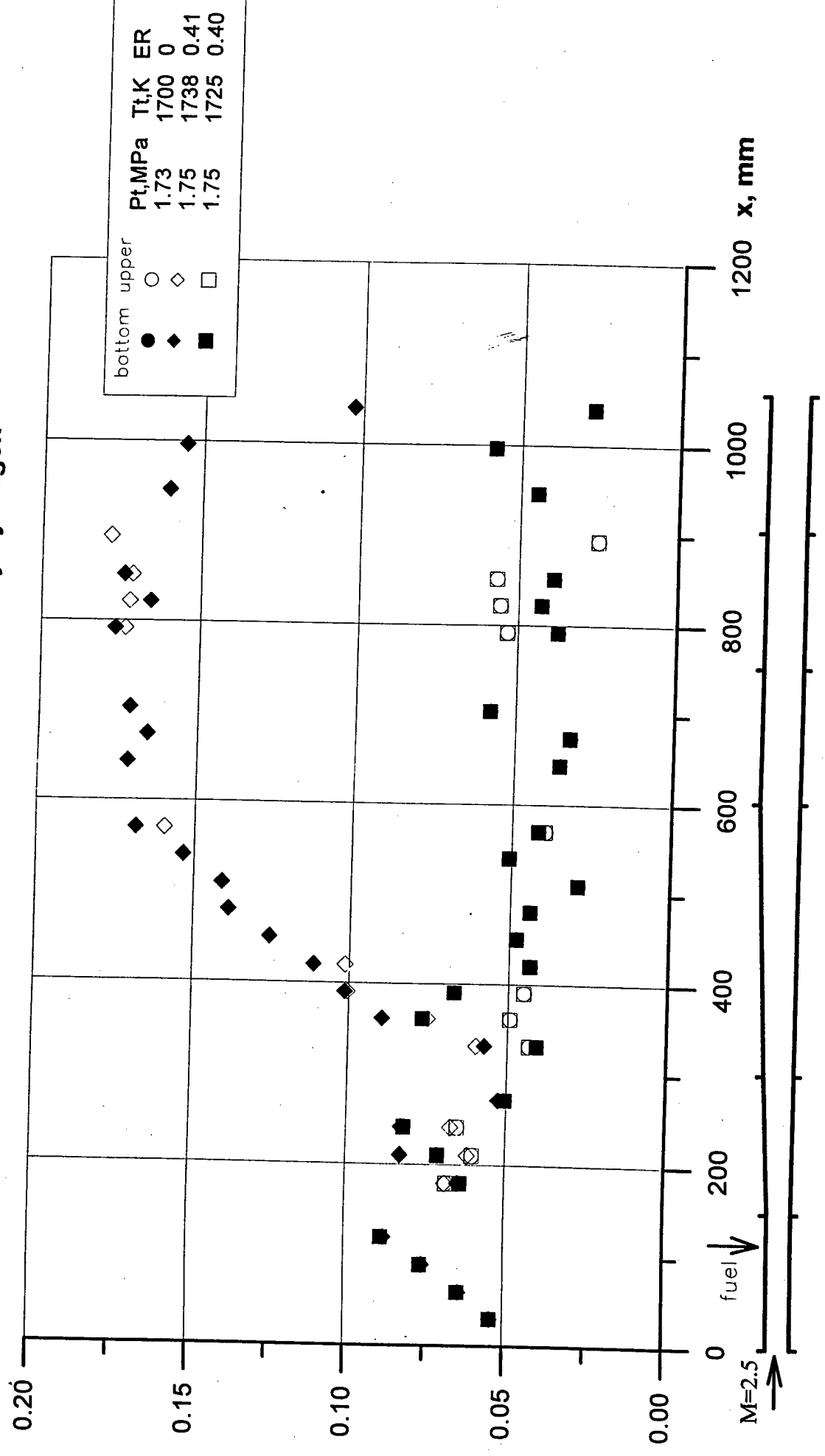


Fig. 9.

Test N1. aerograms, aeration by air.

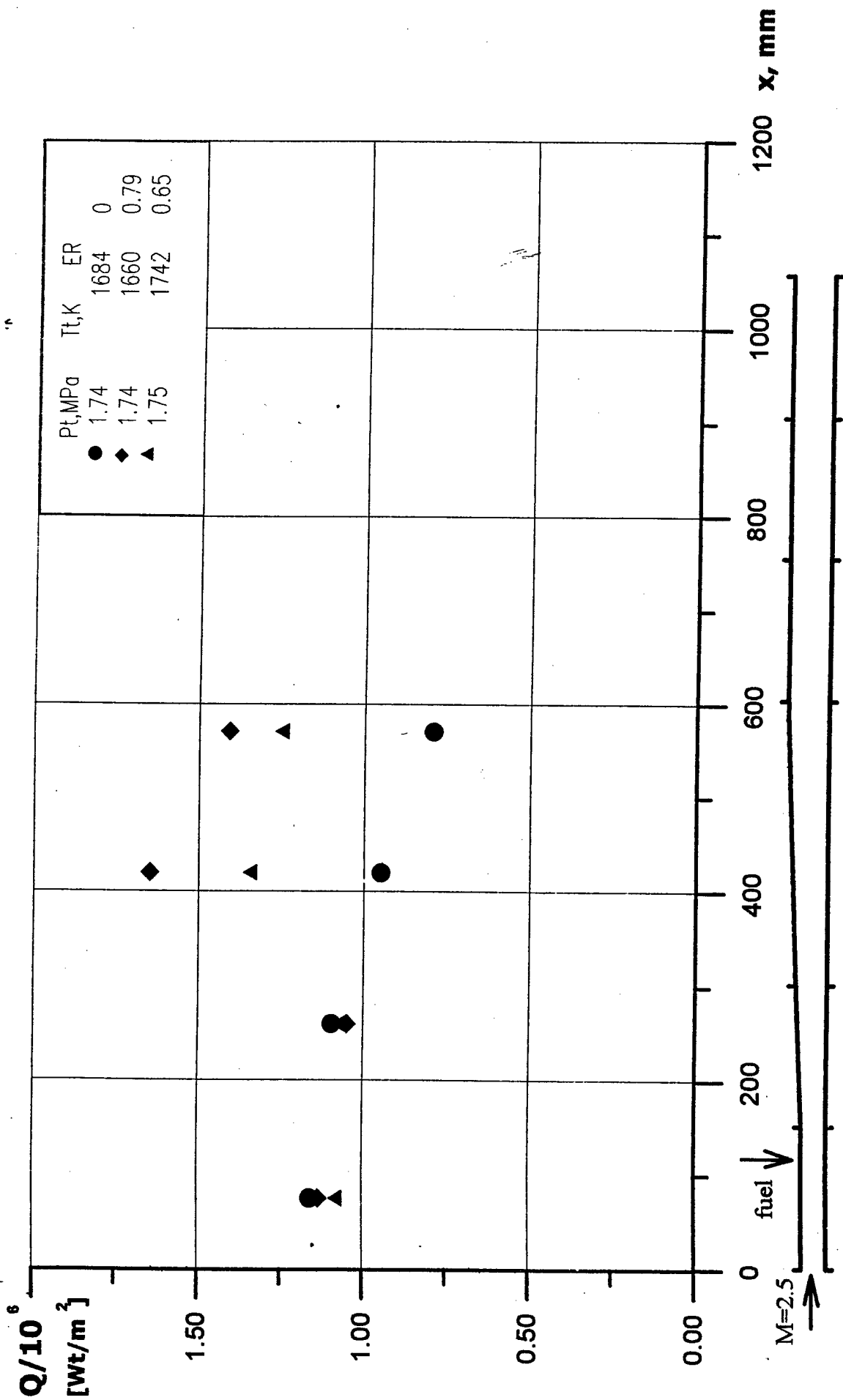


Fig. 10.

Test N5. tubes, aeration by air.

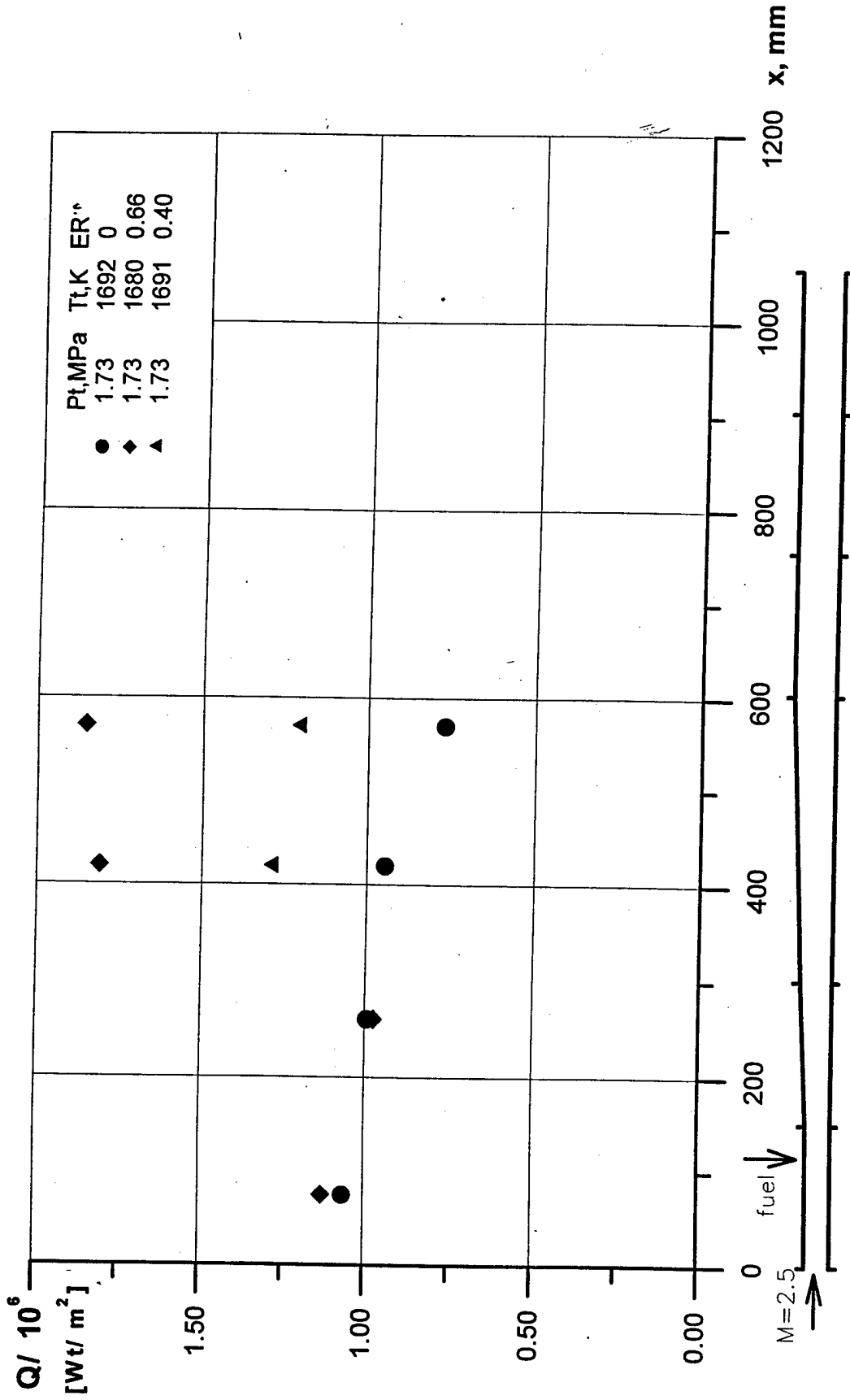
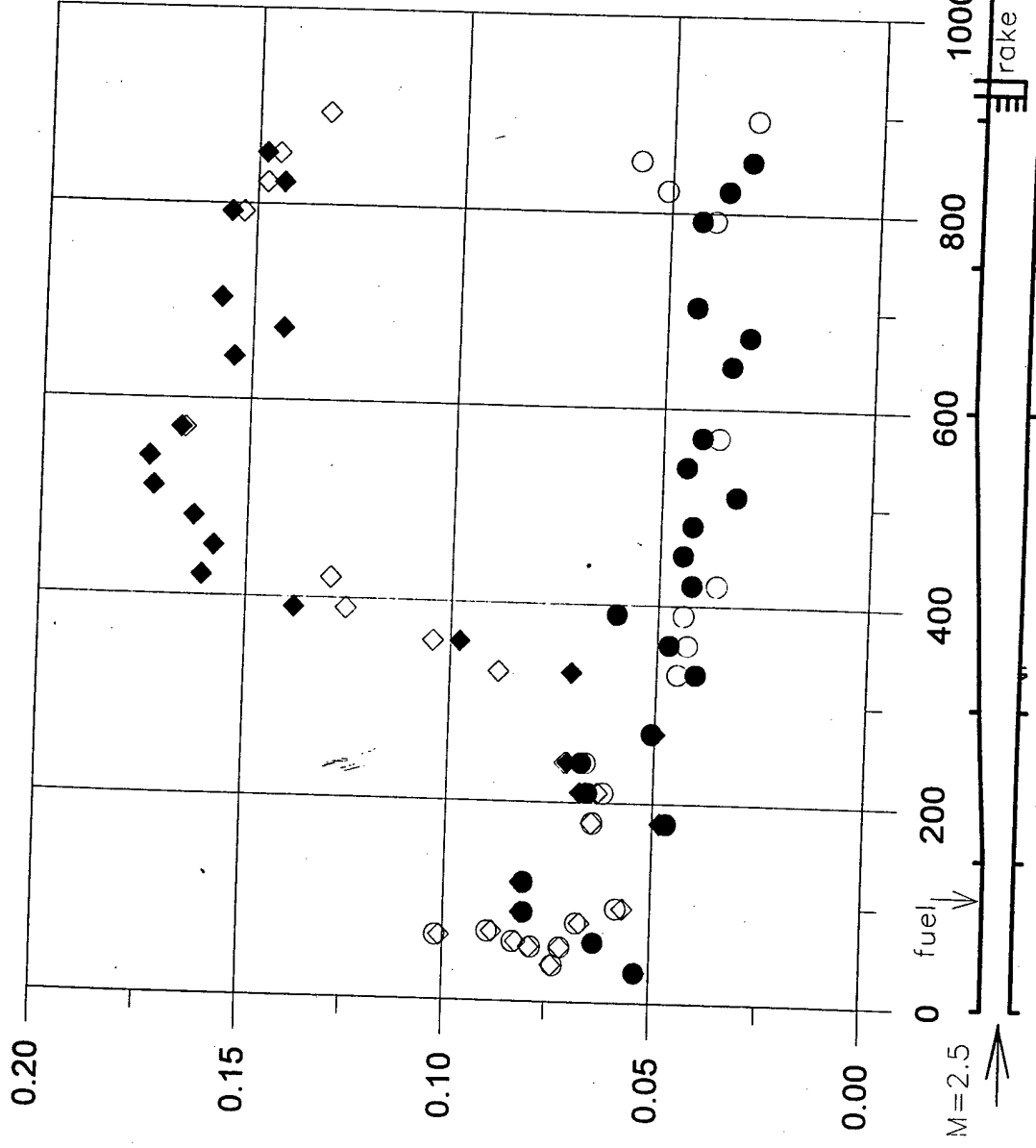


Fig. 11.

**P/Pt** Test No3 aeroramps, aeration by air



bottom	upper	Pt, MPa	Tt, K	ER
●	○	1.78	1752	0
◆	◇	1.78	1741	0.62

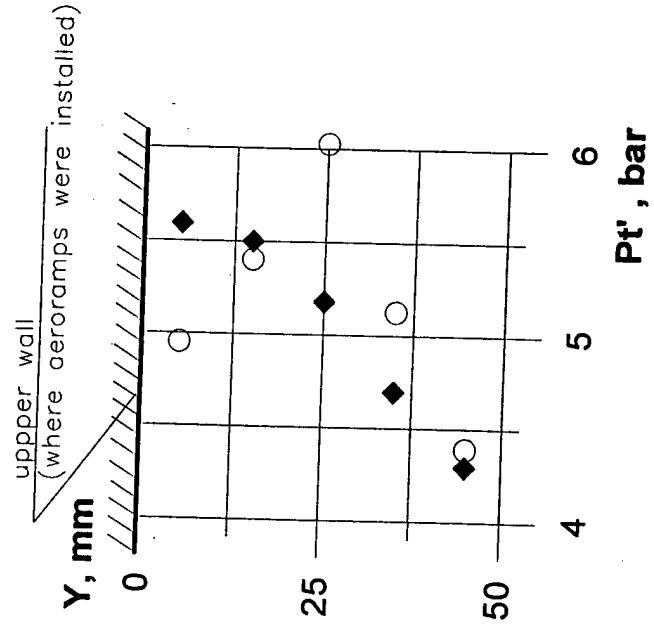


Fig.12.

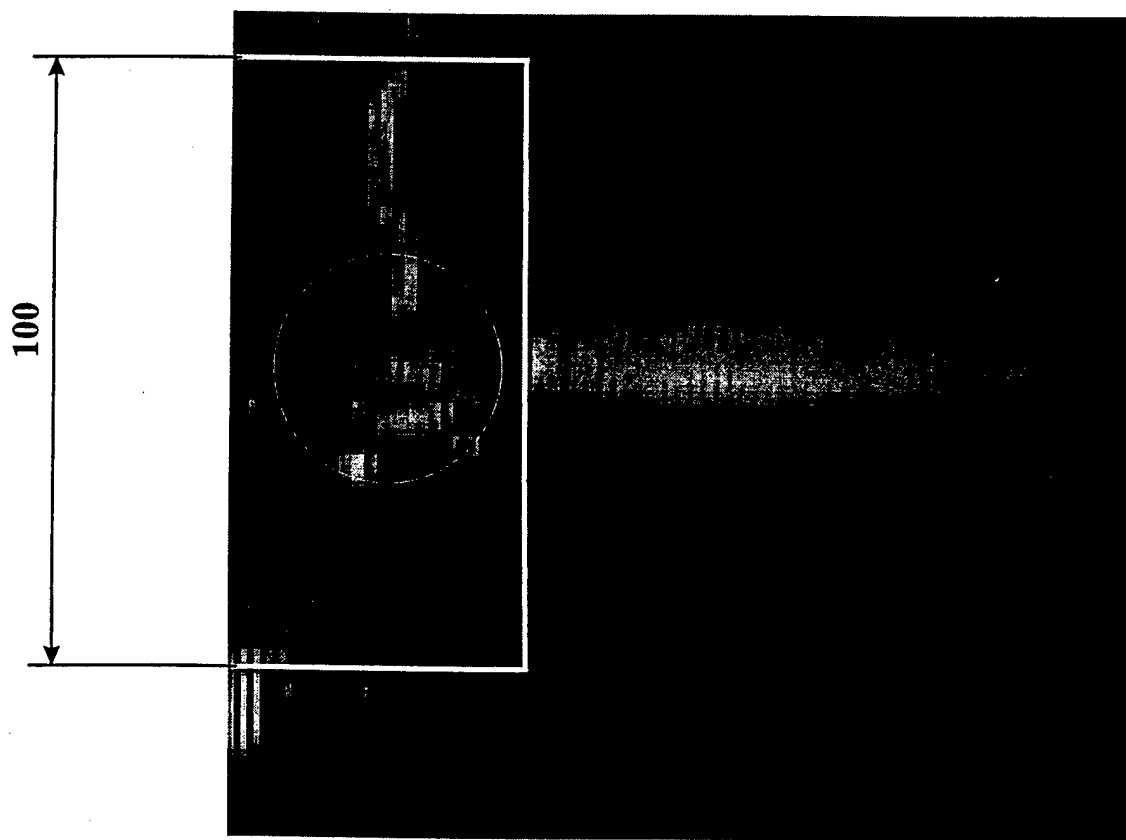
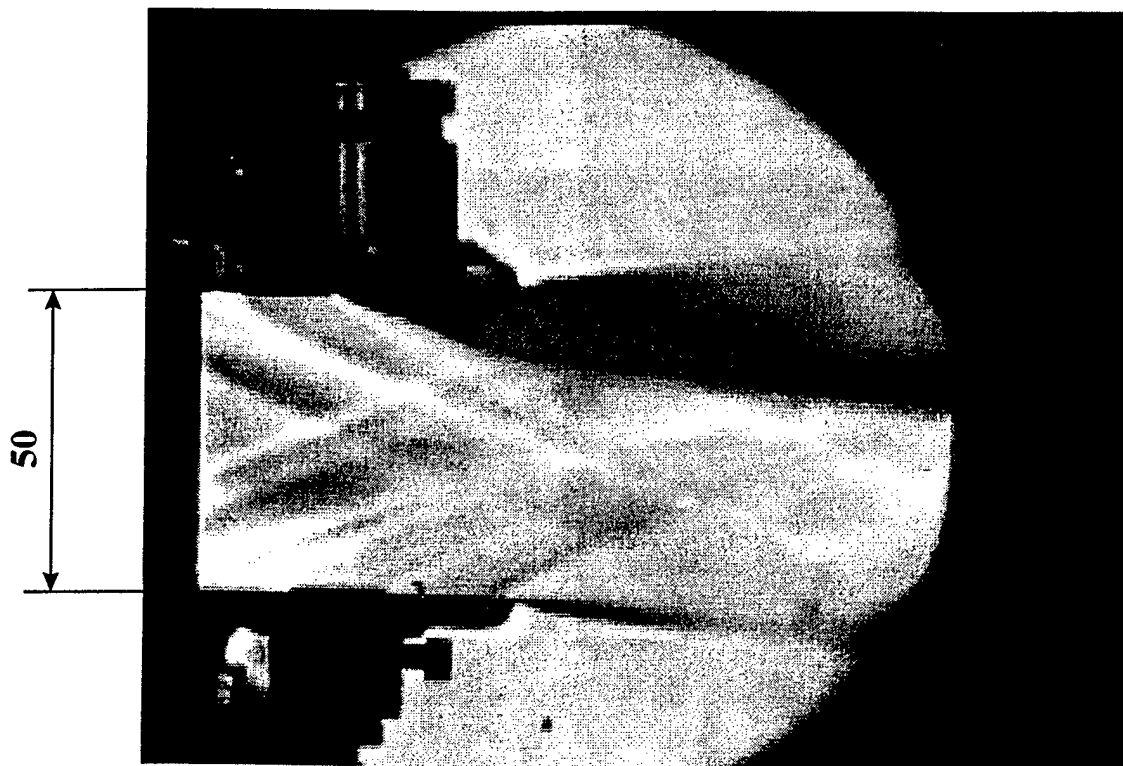


Fig.13.

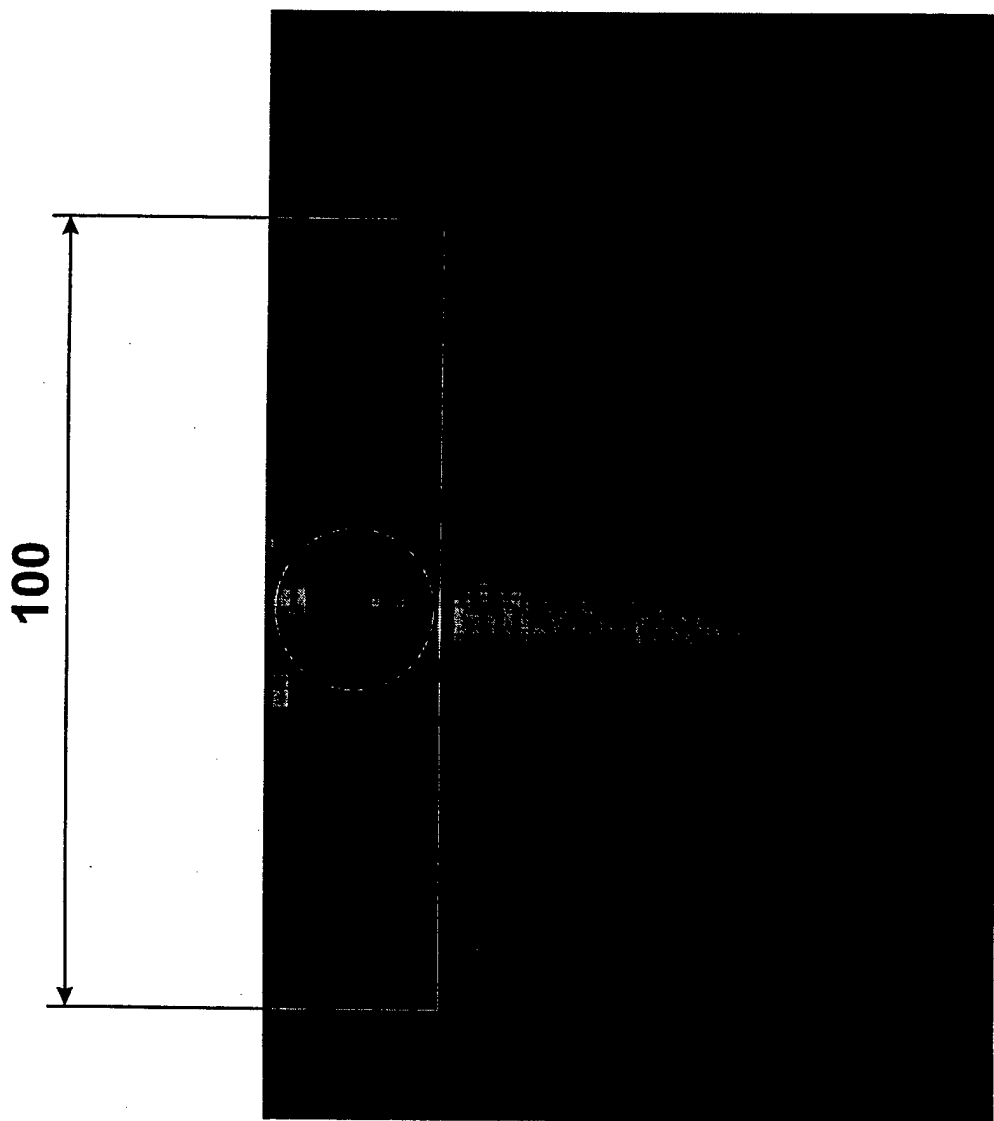
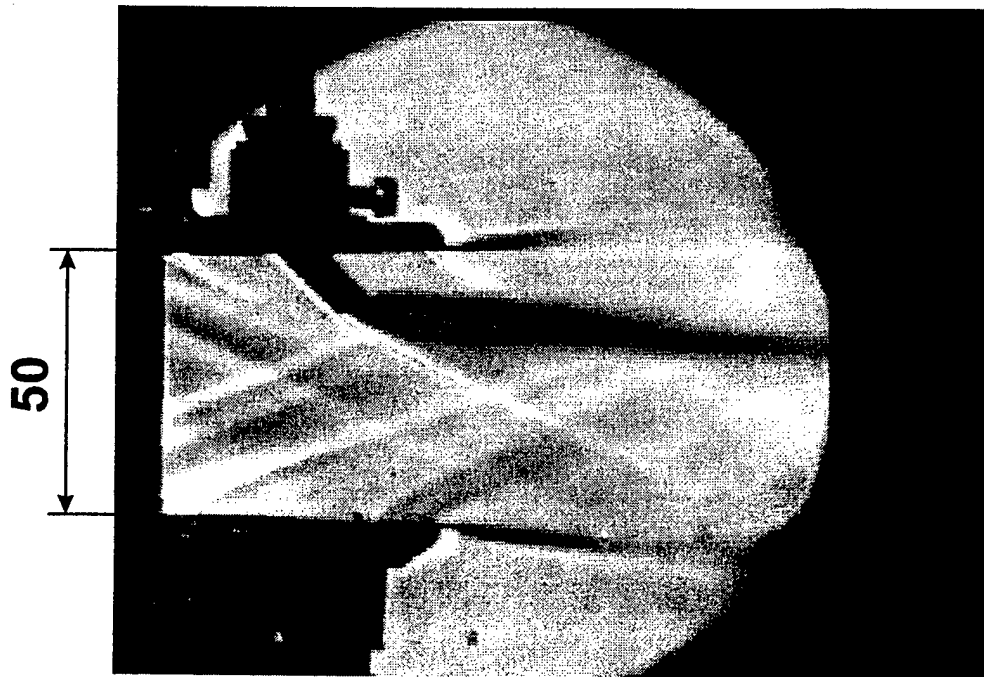


Fig.14.

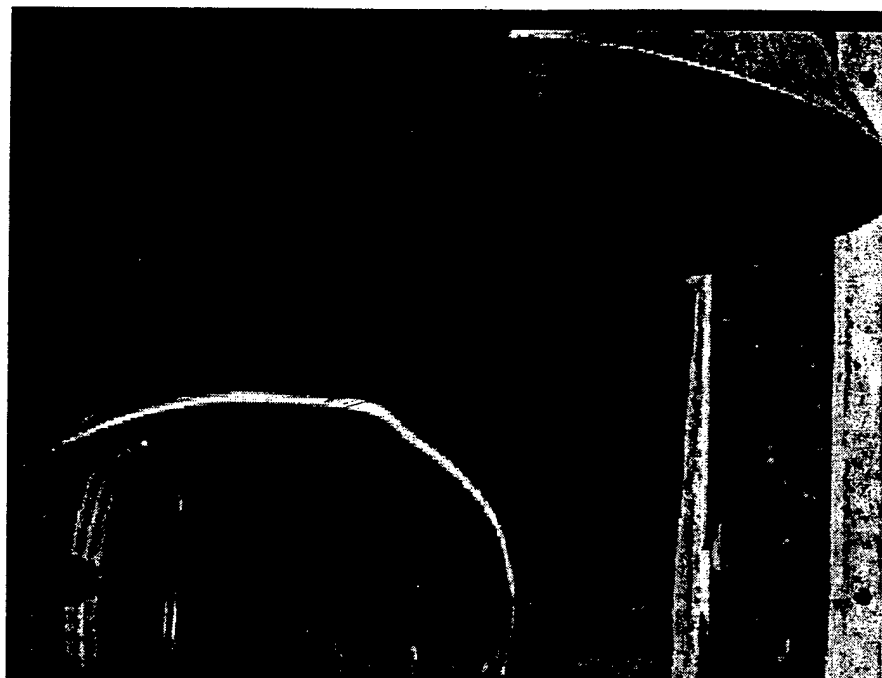
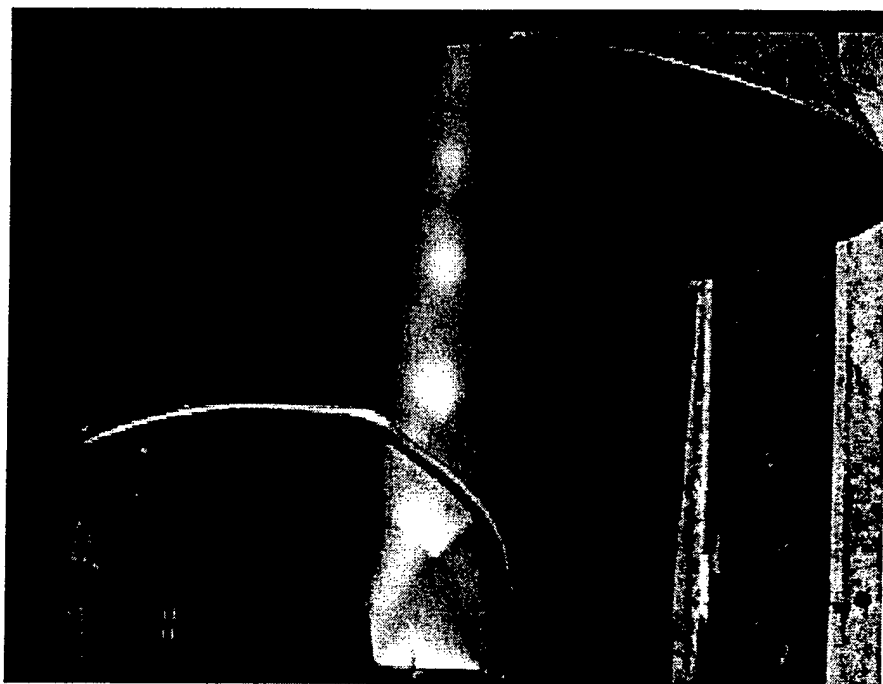


Fig.15.

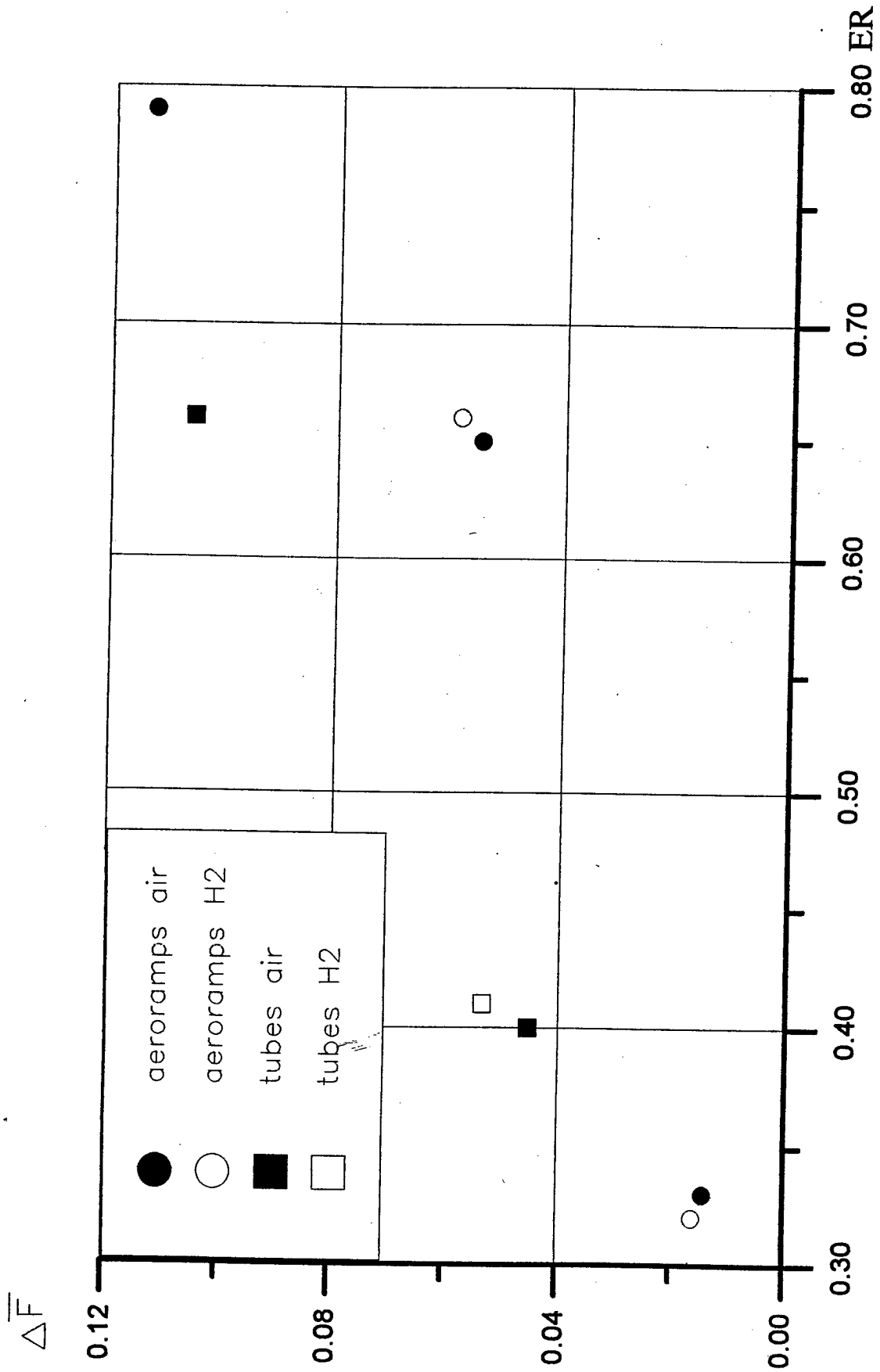


Fig. 16.